Asian Journal of Chemistry; Vol. 34, No. 12 (2022), 3197-3205

ASIAN JOURNAL OF CHEMISTRY

https://doi.org/10.14233/ajchem.2022.24014

Electrochemical Behaviour of Green Synthesized Silver Nanoparticles using *Camellia sinensis* Leaves: Impacts on Photophysical Behaviour of Benzofuran Derivative

SHIVAPRASADAGOUDA PATIL[1,2], MAHANTHESH M. BASANAGOUDA[3], SUDHIR M. HIREMATH[4], S. CHRISTOPHER JEYASEELAN[5], RAGHAVENDRA K. SALI[1,2] and ASHOK H. SIDARAI[1,*]

[1]Department of Studies in Physics, Karnatak University, Dharwad-580003, India
[2]Department of Physics, J.S.S. Arts, Science and Commerce College, Gokak-591307, India
[3]Department of Chemistry, K.L.E. Society's P.C. Jabin Science College, Hubballi-580031, India
[4]Department of P.G. Studies in Physics, KLE Society's J.T. College, Gadag-582101, India
[5]P.G. Department of Physics, Mannar Thirumalai Naicker College, Madurai-625004, India

*Corresponding author: E-mail: ashok_sidarai@rediffmail.com

Received: 9 August 2022; *Accepted*: 27 September 2022; *Published online*: 25 November 2022; AJC-21045

Green synthesis of silver nanoparticles (AgNPs) using *Camellia sinensis* leaf extract was used as a reducing agent. Electrochemical studies of green synthesized AgNPs were investigated using the cyclic voltammetry technique. The effect of modifier composition, scan rate and various concentrations of AgNPs were studied. Photophysical approach of fluorescence emission study of *N*-(2,5-dimethyl-pyrrol-1-yl)-2-(6-methoxy-benzofuran-3-yl)acetamide (DPMBA) dissolved in ethanol. Increasing the concentration of AgNPs decreases the fluorescence intensity and fluorescence lifetime of the DPMBA molecule. This experiment has been carried out at room temperature. The Stern-Volmer (S-V) plot obtained in steady-state and transient state methods. The zeta potential of green synthesized AgNPs was found to be -33.9 mV. This large negative zeta potential represents repulsion among AgNPs and dispersion stability. Furthermore, the computational studies such as molecular docking studies, drug-likeness, Fukui function analysis, molecular electrostatic potential (MEP) and ground state optimized geometry were also conducted. The morphology and particle size of biogenic AgNPs were characterized by transmission electron microscopy (TEM) with electron dispersive X-ray spectroscopy (EDX).

Keywords: *Camellia sinensis*, Silver nanoparticles, Benzofuran derivative, Cyclic voltammetry, Fluorescence quenching.

INTRODUCTION

Benzofuran derivatives have abundant applications in the field of biological and pharmacological fields [1]. In recent years, the broad spectrum of pharmacological activity in individual benzofuran indicates several biological activities like antibacterial, antioxidative, anti-AD, antitumour, anti-parasitic, anti-acetylcholine, anti-inflammatory [1,2] and anti-cancer [3]. Benzofuran derivatives are also used as fluorescent probes to optimize linear and non-linear optical properties [4].

Many researchers have reported the green synthesis of several nanoparticles like gold [5], iron [6] and zinc oxide [7] using *Camellia sinensis* leaves extract. *Camellia sinensis* is popularly known as the tea plant, tea has been prepared by using young leaves, buds and stalks of the plant. Tea contains polyphenolic compounds like catechins, epicatechins, theaflavins, flavonol, glycosides, L-theanine, caffeine, theobromine, these bioactive compounds are responsible for the flavour, aroma, taste and astringency other health beneficial effects [8].

Opportunities in a variety of technologies that use photophysical processes boosted by this light-matter interaction arising due to the high interaction of electromagnetic field with metal nanoparticles. It has recently been demonstrated that optically stimulated metal nanoparticles may initiate chemical changes on their surfaces, in addition to photophysical activities [9]. When compared to phonon-driven thermal processes, the photophysical, exciton processes on metal nanoparticles display fundamentally different behaviour and may allow for selective bond activation. Herein, we explore the photophysical investigation of *N*-(2,5-dimethyl-pyrrol-1-yl)-2-(6-methoxybenzofuran-3-yl)-acetamide (DPMBA) with green synthesized AgNPs as quenchers also for the lifetime measurement of DPMBA molecule.

EXPERIMENTAL

N-(2,5-Dimethyl-pyrrol-1-yl)-2-(6-methoxy-benzofuran-3-yl)acetamide (DPMBA) is a fused molecule of pyrrole and benzofuran derivative was synthesized based on the literature [10]. Ethanol as solvent obtained from S.D. Fine Chemicals Ltd. as of spectroscopic grade. All the measurements were carried out at room temperature.

Preparation of *Camellia sinensis* leaves extract: Fresh *Camellia sinensis* leaves (10 g) were cut into small pieces, chopped and then mixed with 100 mL of distilled water and left for 15 min. The cooled leaf broth solution was filtered through Whatman filter paper and stored in ice cubes.

Green synthesis of silver nanoparticles: Green synthesis of AgNPs has been carried out based on the literature with some modifications [11]. The *Camellia sinensis* leaves extract solution (10 mL) was added dropwise to 0.01 M of $AgNO_3$. This mixture was stirred well with the help of a magnetic stirrer for 5 min, colour changes from pale yellow to dark brown indicating the formation of AgNPs. This mixture was added to 50 mL of Teflon made autoclave which was heated to 160 ºC for 6 h and then cooled to room temperature. After collecting the mixture from the autoclave, separation was done by centrifugation at the rate of 3000 rpm for 15 min, AgNPs were obtained.

Photophysical method: The absorption and emission spectra were recorded on UV-visible spectrophotometer (Hitachi U-3310, Japan) and fluorescence spectrophotometer (Hitachi F-7000, Japan), fluorescence lifetime measurement using time correlated single-photon counting technique [TCSPC ISS model: 90021]. All the measurement were recorded at room temperature.

Electrochemical method: The electrochemical behaviour of AgNPs was studied by cyclic voltammetry (CV). The CV measurement of AgNPs modified carbon paste electrode (CPE) was carried out using Model CH1112C (Version 9.03, USA).

Computational method: The computational studies are performed using Gaussian 09w software along with the DFT method and B3LYP/6-311++G (d, p) basis set [12]. Gauss View 5.0 software [13] molecular docking calculations were done by Auto Dock Vina software.51 and Drug likeness calculations were carried out with the help of the SwissADME [14].

RESULTS AND DISCUSSION

Photophysical approach

Fluorescence quenching of DPMBA molecule using AgNPs: In fluorescence quenching variety of molecular interactions take place which includes excited state reactions, molecular re-arrangements, energy transfer, ground-state complex formation and collisional quenching [15]. Moreover, Stern-Volmer gives relation about the kinetics of a photophysical intermolecular deactivation process. The change in the fluorescence intensity and fluorescence lifetime of DPMBA molecule by adding different concentrations of green synthesized AgNPs.

For steady-state:

$$\frac{F_o}{F} = 1 + K_{SV}[Ag] \quad (1)$$

For transient state:

$$\frac{\tau_o}{\tau} = 1 + K_{SV}[Ag] \quad (2)$$

where F_o = Fluorescence intensity of solute without a quencher; F = Fluorescence intensity of solute with a quencher; τ_o = fluorescence lifetime of solute without a quencher; τ = fluorescence lifetime of solute with a quencher and [Ag] = concentration of silver nanoparticles.

Fluorescence emission and fluorescence lifetime decay measurement of DPMBA molecule in ethanol with adding different concentrations of AgNPs *i.e.* 0.0, 1.3, 2.6, 4.0 and 5.3 µM/L were recorded at room temperature. The increased AgNPs concentration decreases its fluorescence intensity as shown in Fig. 1. This states that fluorescence quenching of DPMBA molecules using AgNPs is purely dynamic. The fluorescence lifetime of DPMBA molecule decreases with adding different concentrations of AgNPs as shown in Fig. 2. A plot of F_0/F and τ_o/τ *versus* [Ag] in steady-state and transient state method according to S-V relation (eqns. 1 and 2) F_o/F and τ_o/τ values are given in Table-1. The linearity of the graph is shown in Fig. 3 and a strong correlation coefficient of 0.95 and 0.87 was obtained.

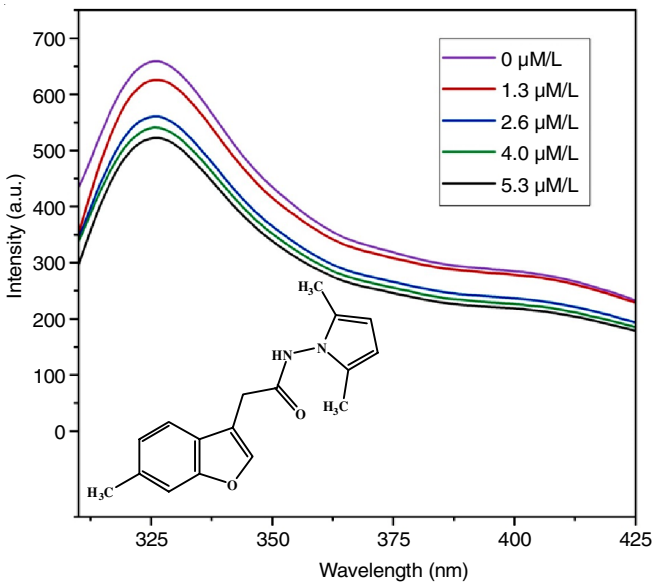

Fig. 1. Fluorescence quenching of DPMBA molecule using green synthesized Ag NPs

Electrochemical approach

Effect of scan rate and concentration: Green synthesized silver nanoparticles (0.020 g) dissolved in 5 mL of ethanol was prepared and kept for sonication for up to 30 min. The experimental setup was carried out in 0.1 M of NaOH solution. Fig. 4 shows the cyclic voltammetric response of bare CPE with modified AgNPs-CPE at a scan rate of 50 mV/s bare CPE has shown a redox peak, in addition to AgNPs-CPE shows a sharp peak shifted in more positive current and compared to bare, AgNPs is a substantial enhancement in the current response.

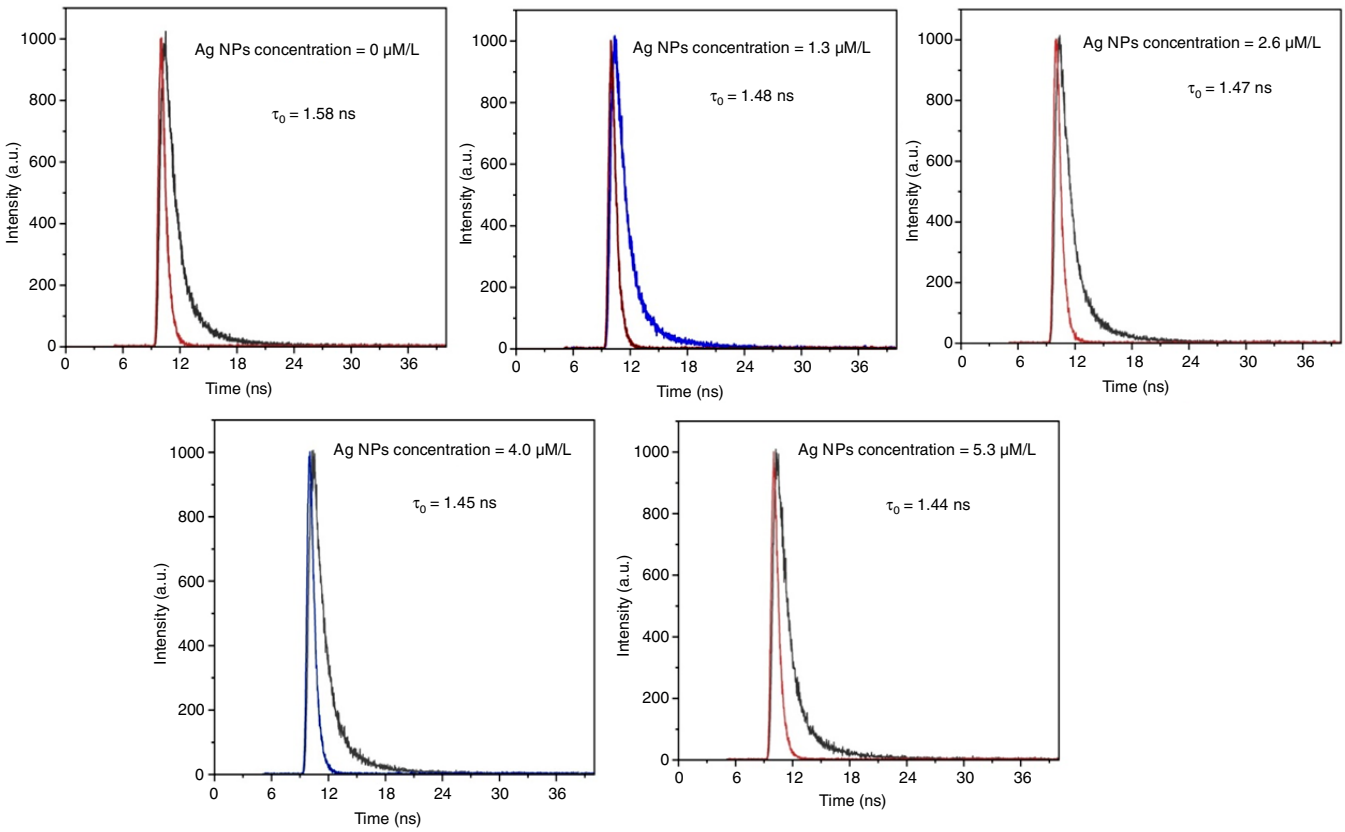

Fig. 2. Life time measurement of DPMBA molecule with different concentration of biogenic Ag NPs

TABLE-1
FLUORESCENCE INTENSITY AND FLUORESCENCE LIFETIME VALUES OF DPMBA MOLECULE IN ETHANOL FOR DIFFERENT CONCENTRATION OF Ag NPs

Ag NPs concentration (μM/L)	Fluorescence lifetime of DPMBA molecule (ns)	τ_0/τ	Fluorescence intensity of DPMBA molecule (a.u.)	F_0/F
0.0	1.58		659.3	
1.3	1.48	1.067	625.6	1.05
2.6	1.47	1.006	590	1.06
4.0	1.45	1.013	550	1.07
5.3	1.44	1.006	500	1.10

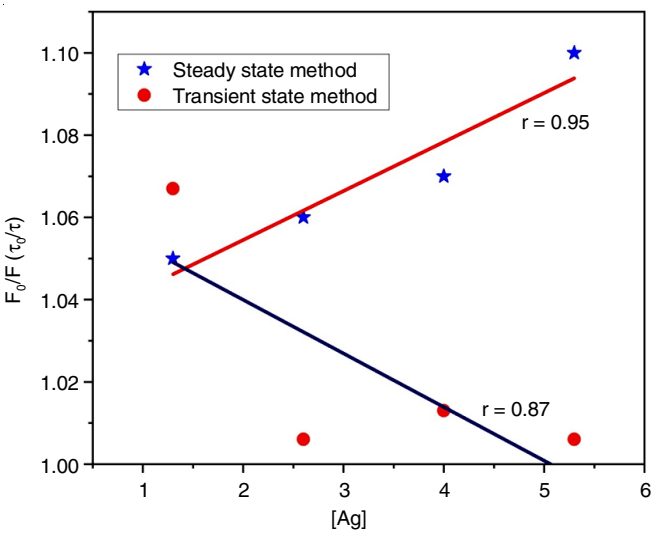

Fig. 3. Steady state and transient state method

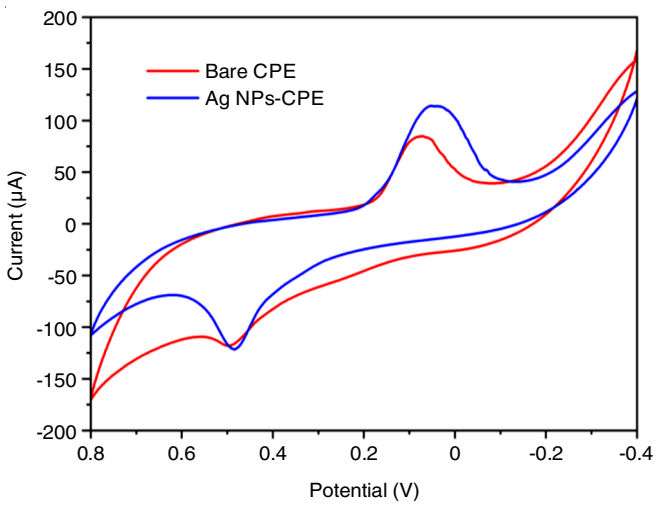

Fig. 4. Electrochemical study of Ag NPs–CPE and Bare CPE was performed in 0.1 NaOH solution

Electrochemical investigation of AgNPs was studied by cyclic voltammetry technique, where three electrodes were used *i.e.* CPE was used as the working electrode, Ag/AgCl as the reference electrode and platinum used as the counter electrode. Effective scan rates in the range of 50 to 170 mV/s and the potential range of 0.8 V to -0.4 V *vs.* Ag/AgCl by varying as shown in Fig. 5. An increase in the scan rates resulted in the shifts of peak potential to the more positive and the effect of scan rates increases, increase in the peak currents, suggesting a diffusion-controlled process (Table-2). A linear plot of peak currents against various scan rates for anodic (Ip_a) peak lines with r = 0.95 (Fig. 6) confirmed the diffusion-controlled process. As AgNPs concentration increases from 4 to 6 µL, its cathodic and anodic peak current are shown in Fig. 7.

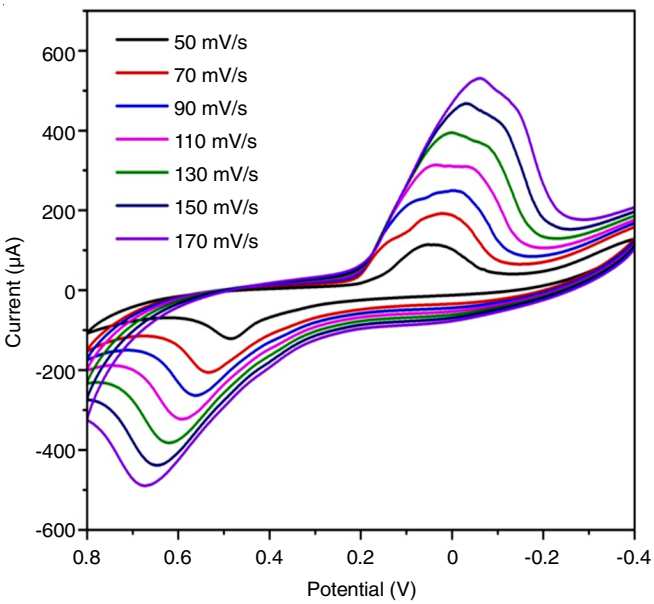

Fig. 5. Addition of 20 mV/s for each scan rate in presence of Ag NPs in 0.1 M NaOH solution

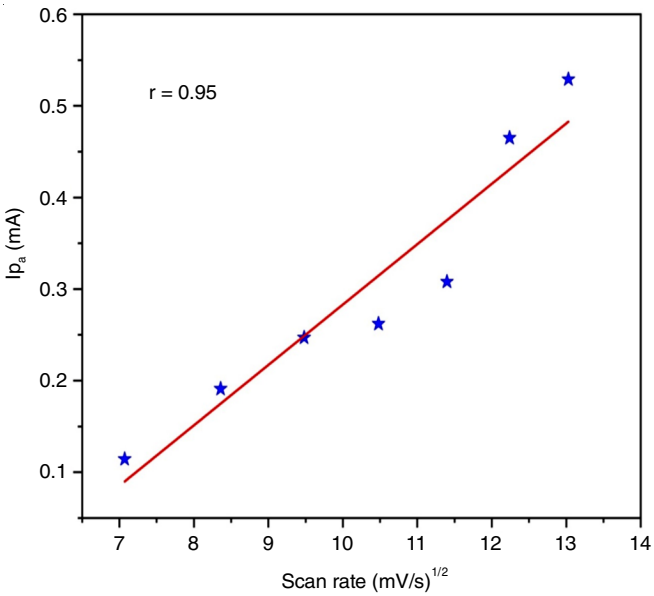

Fig. 6. Anodic peak potential current (Ip_a) with different scan rate squares

TABLE-2
DIFFERENT SCAN RATE AND CURRENT PEAK VALUES

Scan rate (mV/s)	(Scan rate)$^{1/2}$	I_{pa} (mA)
50	7.07	0.1143
70	8.36	0.1911
90	9.48	0.2473
110	10.48	0.2628
130	11.40	0.3083
150	12.24	0.4657
170	13.03	0.5293

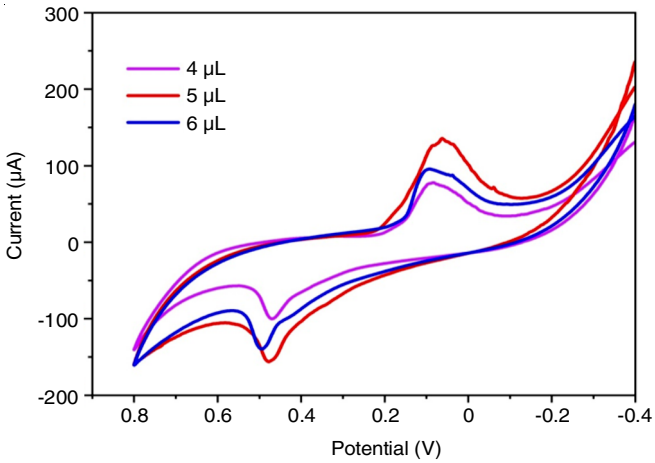

Fig. 7. Addition of Ag NPs concentration *vs.* potential

Computational approach

Molecular electrostatic potential (MEP): Herein, red colour indicates electrophilic, blue colour indicates nucleophilic region MEP chart of DPMBA molecule lies in between -0.02384 a.u (dark red) to 0.02384 a.u (dark blue) as displayed in Fig. 8, while the optimized geometry of DPMBA is shown in Fig. 9. Highest occupied molecular orbital (HOMO) and lowest unoccupied molecular orbital (LUMO) as shown in Fig. 10.

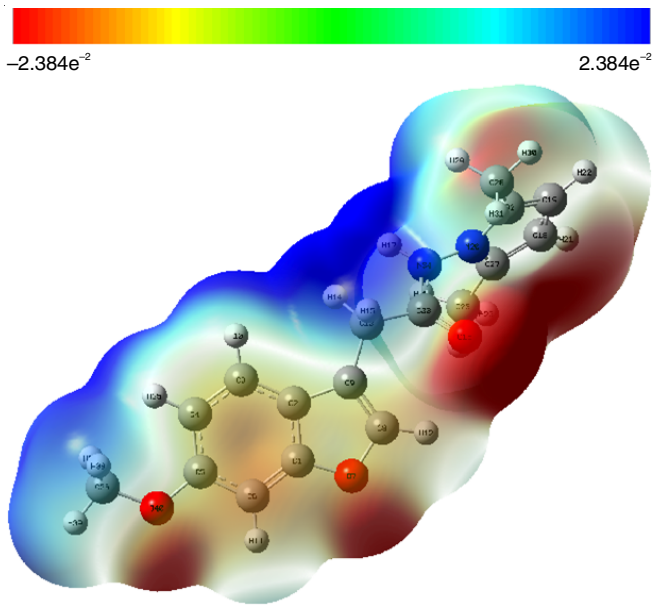

Fig. 8. Molecular electrostatic potential of DPMBA

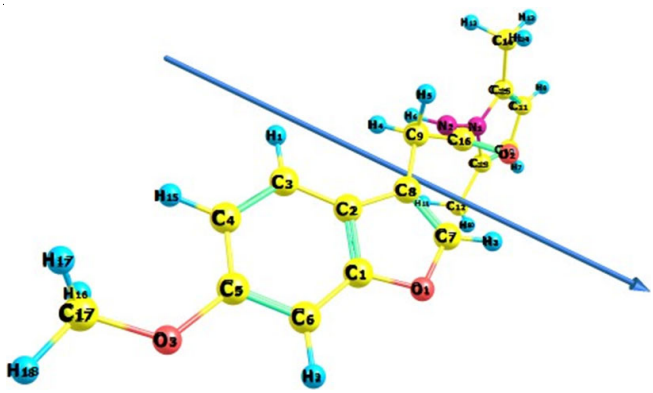

Fig. 9. Ground state optimized geometry structure of DPMBA

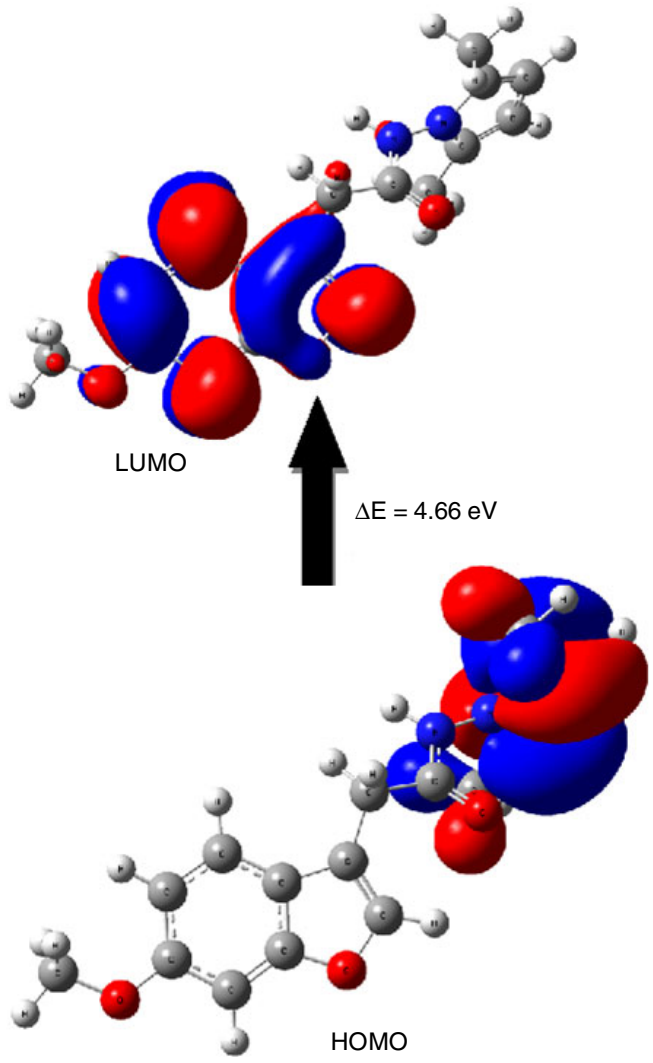

Fig. 10. HOMO and LUMO structure of DPMBA

Molecular docking studies: Benzofuran derivatives gained special interest due to their inhibitory effect against α-glucosidase and protein tyrosine phosphatases, which causes Type 2 diabetes mellitus (T2DM) [16,17]. A molecular docking study was carried out to spot the influence of benzofuran derivatives against α-glucosidase protein and protein tyrosine phosphatases, which causes T2DM.

α-Glucosidase [PDB ID: 3A4A] is a membrane bound enzyme in the intestine, which hydrolyses oligosaccharides and polysaccharides to D-glucose [18-20]. Inhibition of α-glucosidase can retard the release of glucose from complex carbohydrates and therefore can be an important strategy to control type-2 diabetes. Protein tyrosine phosphatases 1B (PTP 1B) enzyme is responsible for selective dephosphorylation of tyrosine residues. Deregulation of PTP 1B [PDB ID: 4ZZH] activity causes type 2 diabetes.

The target proteins were obtained from the PDB format (httb://www.rscb.org.pdb). The optimized molecular structure of the DPMBA molecule was used to generate the ligand PDB file. The Lamarckian genetic algorithm (LGA) was used for molecular docking calculations in the Auto Dock Vina software.51 Docked ligand conformation parameters were analyzed in terms of binding energy, inhibition constant and intermolecular energy of the molecule concerning the targeted proteins and are listed in Table-3. The preferred binding orientations of the BICA ligand with various targeted proteins are shown in Fig. 11, while the ligplot of PTP 1B and α-glucosidase DPMBA molecules is shown in Fig. 12.

Drug likeness studies: Drug likeness analysis is very important in drug design and the drug-likeness variables and bioavailability score of the DPMBA molecule were calculated and given in Table-4. The drug-likeness calculations were carried out with the help of the SwissADME web page [14]. From literature [21], it was analyzed that the values of H-bond acceptor (HBA) and H-bond donor (HBD) values should be less than 10 and 5, respectively. The maximum value of topological polar surface area (TPSA) was 140 $Å^2$ and for DPMBA it was calculated as 56.40 $Å^2$. The value of MR lies in the range of 40 and 130. The MR value of the DPMBA molecules was 85.17. The high GI absorption side, skin permeability (log Kp) was observed as -5.96 cm/s for DPMBA molecules (Table-2). Additionally, the bioavailability of DPMBA molecules is shown in Fig. 13. It was observed that the DPMBA molecule is working in the bioavailability radar and thus found to have a good physico-chemical profile.

Fukui function analysis: The charge densities of DPMBA molecule of its cation and anion were calculated in a doublet state but have the same geometry as singlet state neutral molecule.

TABLE-3
OBTAINED DOCKING PARAMETERS OF THE MOLECULE *N*-(2,5-DIMETHYL-PYRROL-1-YL)-2-(6-METHOXY-BENZOFURAN-3-YL)-ACETAMIDE [DPMBA] ON THEIR RANK CALCULATED BY AUTODOCK

Target protein (receptor)	Protein (PDB ID)	Docking parameters based on the rank								
		Binding energy (Kcal/mol)			Estimated inhibition constant (μm)			Intermolecular energy (Kcal/mol)		
		1	2	3	1	2	3	1	2	3
PTP 1B	4ZZH	-5.70	-5.60	-5.38	65.87	78.05	114.71	-6.90	-6.80	-6.57
α-Glucosidase	3A4A	-5.54	-5.53	-5.39	86.91	88.81	111.79	-6.73	-6.72	-6.68

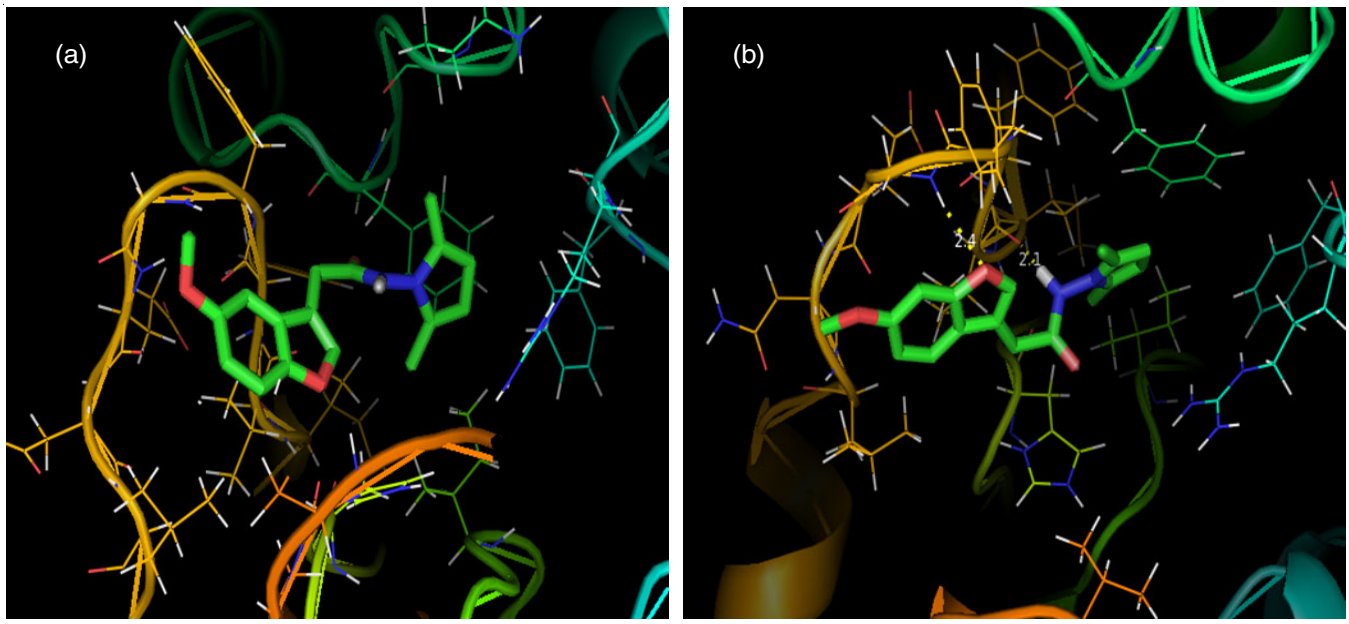

Fig. 11. Lowest energy docked poses of the PTP 1B with (a) DPMBA (b) α-glucosidase

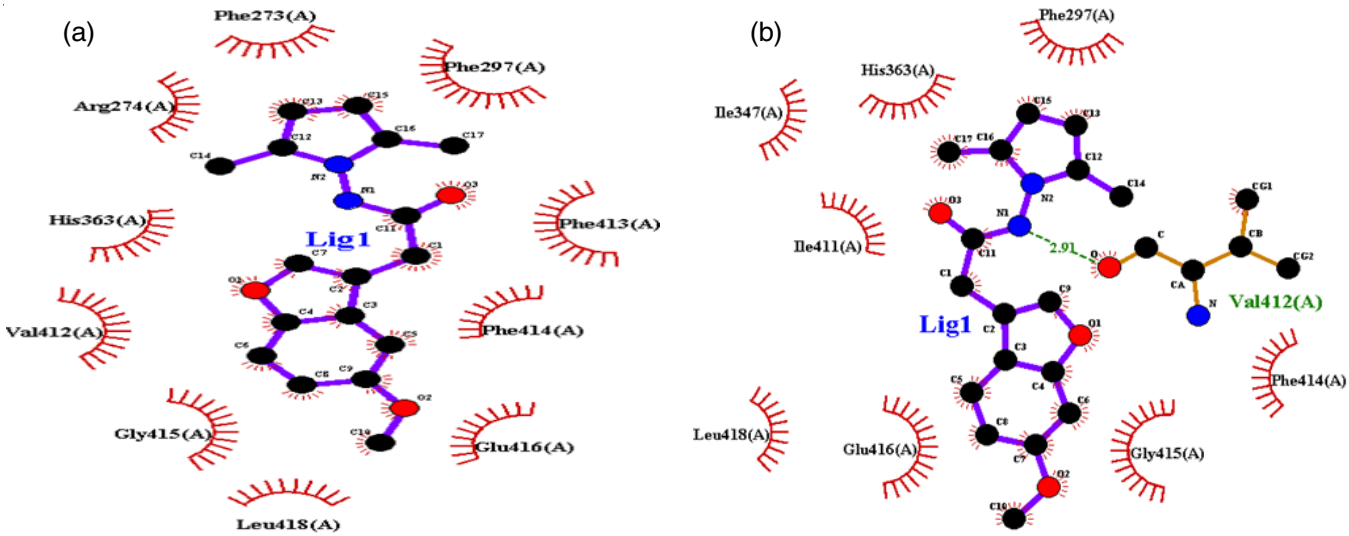

Fig. 12. Ligplot diagrams of the binding modes of DPMBA ligands with (a) PTP 1B, (b) α-glucosidase

TABLE-4
DRUG LIKENESS PROPERTIES OF DPMBA

Drug likeness properties	DPMBA
Hydrogen bond donor (HBD)	1
Hydrogen bond acceptor (HBA)	3
Molar refractivity (MR)	85.17
Topological polar surface area (TPSA Å^2)	56.40
Gastrointestinal (GI) absorption	High
Blood-brain barrier (BBB) penetration	-5.96
Skin permeability (Log Kp (cm/s))	-5.96
Bioavailability	0.55
Lipinski rule violation	0

The Fukui functions for (f_k^+, f_k^-, f_k^0 and Δf) for atomic sites in DPMBA are listed in Table-5. The dual descriptor (Δf) is an important reactivity descriptor, which more efficiently predicts the reactive sites of a molecule. The site is favoured for a nucleophilic attack is given by Δf(r) > 0 and the site favoured

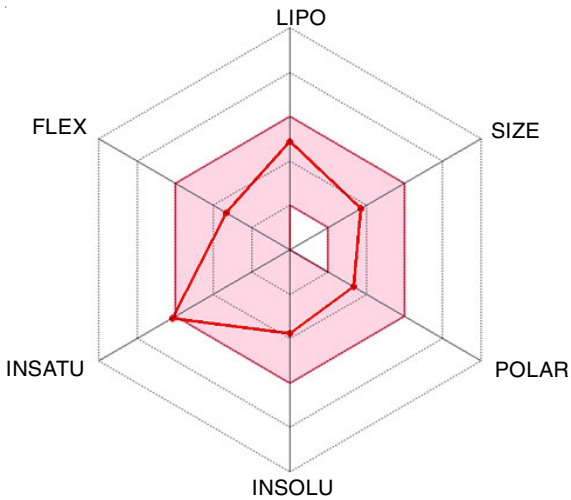

Fig. 13. Bioavailability radars of DPMBA

TABLE-5
LOCAL REACTIVITY DESCRIPTORS OF DPMBA

Atom	Mulliken atomic charge			Fukui functions			$\Delta f = f_k^+ - f_k^-$
	Neutral q(N)	Cation q(N-1)	Anion q(N+1)	Nucleophilic attack (f_k^+)	Nucleophilic attack (f_k^+)	Nucleophilic attack (f_k^+)	
C1	0.1831	0.1706	0.1896	-0.0125	-0.0065	-0.0095	-0.0060
C2	0.0253	0.0278	0.0329	0.0026	-0.0077	-0.0025	0.0102
C3	-0.1531	-0.2243	-0.1293	-0.0711	-0.0238	-0.0475	-0.0473
C4	-0.1471	-0.1642	-0.1289	-0.0171	-0.0182	-0.0177	0.0011
C5	0.2677	0.2305	0.2806	-0.0372	-0.0129	-0.0251	-0.0242
C6	-0.0965	-0.1667	-0.0619	-0.0702	-0.0346	-0.0524	-0.0356
O7	-0.5171	-0.5520	-0.4884	-0.0349	-0.0287	-0.0318	-0.0063
C8	0.0645	-0.0156	0.1052	-0.0800	-0.0407	-0.0604	-0.0393
C9	0.0771	0.0626	0.0785	-0.0145	-0.0014	-0.0079	-0.0130
H10	0.1251	0.0355	0.1627	-0.0896	-0.0376	-0.0636	-0.0520
H11	0.1595	0.0732	0.2078	-0.0863	-0.0482	-0.0673	-0.0381
H12	0.1987	0.1224	0.2323	-0.0762	-0.0337	-0.0549	-0.0426
C13	-0.3781	-0.3726	-0.3796	0.0055	0.0015	0.0035	0.0040
H14	0.1406	0.1126	0.1595	-0.0280	-0.0188	-0.0234	-0.0092
H15	0.1954	0.1548	0.2266	-0.0406	-0.0312	-0.0359	-0.0094
O16	-0.4228	-0.4386	-0.4044	-0.0158	-0.0184	-0.0171	0.0026
H17	0.3371	0.3117	0.3566	-0.0254	-0.0195	-0.0224	-0.0058
C18	-0.2112	-0.2204	-0.1837	-0.0092	-0.0275	-0.0183	0.0183
C19	-0.2107	-0.2193	-0.1839	-0.0086	-0.0268	-0.0177	0.0181
N20	-0.5676	-0.5656	-0.5753	0.0021	0.0077	0.0049	-0.0056
H21	0.1188	0.0901	0.1846	-0.0287	-0.0658	-0.0472	0.0371
H22	0.1186	0.0883	0.1848	-0.0302	-0.0663	-0.0482	0.0361
C23	-0.4566	-0.4525	-0.4633	0.0040	0.0067	0.0054	-0.0027
H24	0.1656	0.1753	0.1936	0.0097	-0.0279	-0.0091	0.0376
H25	0.1565	0.1315	0.1945	-0.0250	-0.0380	-0.0315	0.0130
H26	0.1371	0.1323	0.1774	-0.0048	-0.0403	-0.0225	0.0355
C27	0.3811	0.3771	0.4198	-0.0040	-0.0388	-0.0214	0.0348
C28	-0.4571	-0.4532	-0.4643	0.0039	0.0072	0.0056	-0.0033
H29	0.1354	0.1277	0.1774	-0.0077	-0.0419	-0.0248	0.0343
H30	0.1564	0.1324	0.1943	-0.0240	-0.0379	-0.0309	0.0139
H31	0.1640	0.1624	0.1997	-0.0016	-0.0357	-0.0187	0.0340
C32	0.3819	0.3772	0.4211	-0.0047	-0.0392	-0.0219	0.0345
C33	0.5670	0.5598	0.5613	-0.0072	0.0056	-0.0008	-0.0128
N34	-0.5019	-0.5011	-0.4947	0.0008	-0.0072	-0.0032	0.0079
H35	0.1265	0.0520	0.1674	-0.0746	-0.0409	-0.0577	-0.0337
C36	-0.1685	-0.1321	-0.1985	0.0364	0.0300	0.0332	0.0064
H37	0.1460	0.1151	0.1741	-0.0309	-0.0281	-0.0295	-0.0029
H38	0.1468	0.1156	0.1762	-0.0312	-0.0294	0.2056	-0.1780
H39	0.1695	0.1206	0.2062	-0.0489	-0.0367	0.2429	-0.2185
O40	-0.5570	-0.5811	-0.5084	-0.0241	-0.0486	-0.4598	0.5329

for an electrophilic attack is given by $\Delta f(r) > 0$. The atoms in the DPMBA molecule with $\Delta f_k > 0$ values were predicted in the order of O40 > H24 > H21 > H22 > H22 and these are the possible sites for nucleophilic attack. The atoms with values of $\Delta f_k < 0$ values of CBT were predicted in the order of H39 > H38 > H10 > C3 > H12 and these are the sites favourable for the electrophilic attack. These obtained results help in the identification of nucleophilic and electrophilic regions involve in the protein-ligand interactions.

Zeta potential of synthesized AgNPs: Zeta potential measurement of biosynthesized AgNPs was carried out in an ethanol medium using HORIBA Scientific SZ-100 at 25 ºC and the zeta potential of the green synthesized AgNPs was found to be -33.9 mV (Fig. 14). It is suggested that the surface of the nanoparticles is negatively charged and dispersed in the medium. The negative value confirmed the repulsion among the particles and are very stable. The AgNPs size measurement was calculated using scattering light intensity technique 59.6 nm using ethanol as the dispersion medium.

TEM-EDX analysis: The morphological structure of the biogenic AgNPs was studied using TEM-EDX images obtained by TALOS F200S G2. It was observed that monodispersed and spherical size particles in the range of 30-70 nm and have agglomeration between some particles. The particle histogram showed the average particle size is about 50 nm. Fig. 15 depicts the TEM images of AgNPs of scale range 100 nm and 50 nm, along with TEM, the EDX results spectrum indicates the major elements of C, O, Ag and Na as shown in Fig. 16.

Conclusion

A cost-effective, environment-friendly green synthesis of AgNPs using *Camellia sinensis* leaves extract solution as a

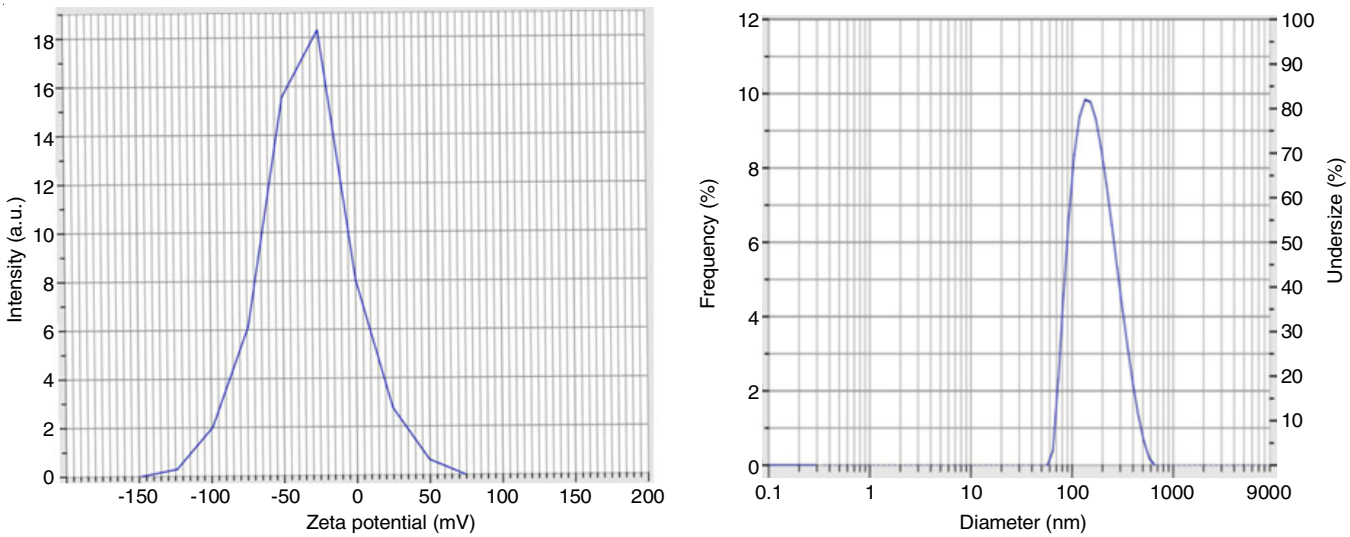

Fig. 14. Zeta potential of Ag NPs

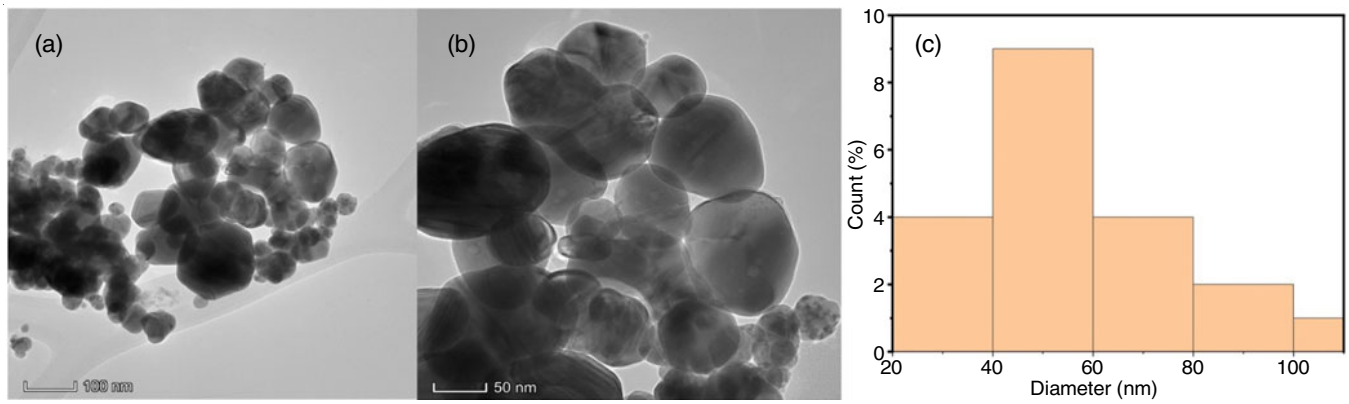

Fig. 15. TEM images of Ag NPs scale range is (a) 100 nm, (b) 50 nm, (c) average diameter of the Ag particle size

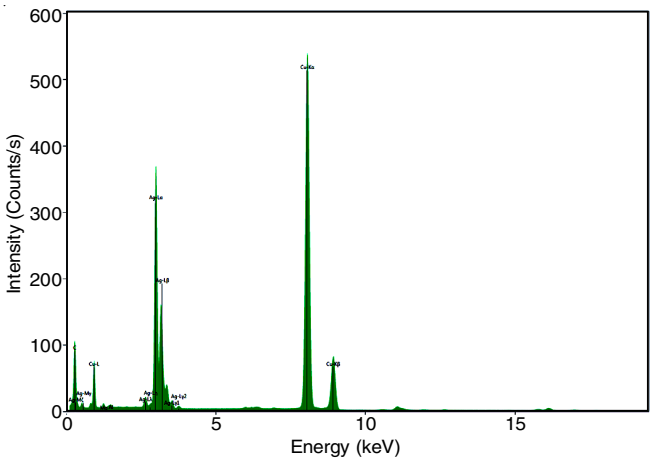

Fig. 16. Elemental mapping TEM-EDX spectrum of Ag NPs

reducing agent. Electrochemical investigation of AgNPs using cyclic voltammetry technique gives stable and active results. The effect of concentration varies and the effect of scan rate leads to a good result. A good correlation coefficient found to be linear for different scan rates is 0.95. The photophysical investigation of *N*-(2,5-dimethyl-pyrrol-1-yl)-2-(6-methoxy-benzofuran-3-yl)acetamide (DPMBA) molecule with green synthesized AgNPs, herein AgNPs are used as quenchers also for the lifetime period of DPMBA molecule. Increasing AgNPs concentration decreases the fluorescence intensity and lifetime measurement of the DPMBA molecule. The Stern-Volmer values were found to be linear and had a good correlation coefficient. The computational investigation of DPMBA molecule has been reported molecular electrostatic potential, optimized geometry structure, molecular docking study, drug-likeness study and Fukui function analysis.

ACKNOWLEDGEMENTS

One of the authors, SP is grateful to Prof. Suresh M. Tuwar for electrochemical studies using cyclic voltammetry technique. Thanks to Prof. M.Y. Kariduraganavar for recording the zeta potential measurement under DST-PURSE Phase-II Project and to the technical staff of USIC, Karnatak University, Dharwad for providing the spectroscopic data.

CONFLICT OF INTEREST

The authors declare that there is no conflict of interests regarding the publication of this article.

REFERENCES

1. Y.-H. Miao, Y.-H Hu, J. Yang, T. Liu, J. Sun and X.-J. Wang, *RSC Adv.*, **9**, 27510 (2019); https://doi.org/10.1039/C9RA04917G
2. H. Khanam and Shamsuzzaman, *Eur. J. Med. Chem.*, **97**, 483 (2015); https://doi.org/10.1016/j.ejmech.2014.11.039
3. J. Farhat, L. Alzyoud, M. Alwahsh and B. Al-Omari, *Cancers*, **14**, 2196 (2022); https://doi.org/10.3390/cancers14092196
4. P. Krawczyk, *J. Mol. Model.*, **26**, 272 (2020); https://doi.org/10.1007/s00894-020-04539-6
5. S.K. Boruah, P.K. Boruah, P. Sarma and C. Medhi, *Adv. Mater. Lett.*, **3**, 481 (2012); https://doi.org/10.5185/amlett.2012.icnano.103
6. G. Ksv, *J. Nanomed. Biotherap. Disc.*, **7**, 1 (2017); https://doi.org/10.4172/2155-983X.1000151
7. S.R. Sethilkumar and T. Sivakumar, *Int. J. Pharm. Pharm. Sci.*, **6**, 461 (2014).
8. S. Samanta, *J. Am. Coll. Nutr.*, **41**, 65 (2022); https://doi.org/10.1080/07315724.2020.1827082
9. S. Linic, U. Aslam, C. Boerigter and M. Morabito, *Nat. Mater.*, **14**, 567 (2015); https://doi.org/10.1038/nmat4281
10. V.S. Negalurmath, Ph.D. Thesis, Synthesis of Some Heterocyclic Compounds and Study of their Biological Activities, Karnatak University, Dharwad, India (2019).
11. S. Ponarulselvam, C. Panneerselvam, K. Murugan, K. Kalimuthu, N. Aarthi and S. Thangamani, *Asian Pac. J. Trop. Biomed.*, **2**, 574 (2012); https://doi.org/10.1016/S2221-1691(12)60100-2
12. M.J. Frisch, G.W. Trucks, H.B. Schlegel, G.E. Scuseria, M.A. Robb, J.R. Cheeseman, J.A. Montgomery Jr., T. Vreven, K.N. Kudin, J.C. Burant, J.M. Millam, S.S. Iyengar, J. Tomasi, V. Barone, B. Mennucci, M. Cossi, G. Scalmani, N. Rega, G.A. Petersson, H. Nakatsuji, M. Hada, M. Ehara, K. Toyota, R. Fukuda, J. Hasegawa, M. Ishida, T. Nakajima, Y. Honda, O. Kitao, H. Nakai, M. Klene, X. Li and J.E. Knox, Gaussian Inc., Wallingford, CT (2004).
13. A.B. Nielsen and A.J. Holder, Gauss View 5.0 User's Reference, Gaussian Inc, Pittsburgh (2009).
14. A. Daina, O. Michielin and V. Zoete, *Sci. Rep.*, **7**, 42717 (2017); https://doi.org/10.1038/srep42717
15. J.R. Lakowicz, Principle of Fluorescence Spectroscopy, Springer, Ed. 3 (2006).
16. T.O. Olomola, M.J. Mphahlele and S. Gildenhuys, *Bioorg. Chem.*, **100**, 103945 (2020); https://doi.org/10.1016/j.bioorg.2020.103945
17. G.L. Delogu, B. Era, S. Floris, R. Medda, V. Sogos, F. Pintus, G. Gatto, A. Kumar, G.T. Westermark and A. Fais, *Int. J. Biol. Macromol.*, **169**, 428 (2021); https://doi.org/10.1016/j.ijbiomac.2020.12.117
18. F. Azimi, H. Azizian, M. Najaf, G. Khodarahmi, M. Hassanzadeh, J.B. Ghasemi, L. Saghaei, M.A. Faramarzi, B. Larijani, F. Hassanzadeh and M. Mahdavi, *Sci. Rep.*, **11**, 20776 (2021); https://doi.org/10.1038/s41598-021-99899-1
19. Z. Xie, G. Wang, J. Wang, M. Chen, Y. Peng, L. Li, B. Deng, S. Chen and W. Li, *Molecules*, **22**, 659 (2017); https://doi.org/10.3390/molecules22040659
20. M. Solangi, Kanwal, K. Mohammed Khan, F. Saleem, S. Hameed, J. Iqbal, Z. Shafique, U. Qureshi, Z. Ul-Haq, M. Taha and S. Perveen, *Bioorg. Med. Chem.*, **28**, 115605 (2020); https://doi.org/10.1016/j.bmc.2020.115605
21. I. Çapan, S. Servi, I. Yildirim and Y. Sert, *ChemistrySelect*, **6**, 5838 (2021); https://doi.org/10.1002/slct.202101086